Chemical Engineering Science, Vol. 41, No. 11, pp. 2931–2938, 1986.
Printed in Great Britain.

0009–2509/86 $3.00 + 0.00
Pergamon Journals Ltd.

PRESSURE SWING ADSORPTION: EXPERIMENTAL STUDY OF AN EQUILIBRIUM THEORY

JOHN C. KAYSER and KENT S. KNAEBEL†
Department of Chemical Engineering, The Ohio State University, Columbus, OH 43210, U.S.A.

(*Received* 28 *May* 1985)

Abstract—A theoretical model of pressure swing adsorption (PSA) processes that is based on local, linear equilibrium of a binary gas mixture with an adsorbent was experimentally tested under conditions supportive of the inherent assumptions and constraints. The components studied were nitrogen, oxygen and argon with 5A zeolite molecular sieve, at temperatures from 20 to 60°C. Simple breakthrough experiments were analysed to predict the slopes of the isotherms within 5.4% (mean absolute error) of actual equilibrium values. In two-bed PSA experiments at pressure ratios from 6.5 to 840, the recoveries of the light component (oxygen and argon) were within 7.1% (mean absolute error) of those predicted by theory. Typically, the feed rate to the process was about 2751 (STP)/kg h, based on the total mass of adsorbent. The light-component product purity averaged 99.6% (based on volume) and was never less than 99.2%, while theory predicts complete separation is possible. The results support the validity of the theoretical model for the conditions of the experiments.

1. INTRODUCTION

Pressure swing adsorption (PSA) is a cyclic process used for the separation of gas mixtures. PSA processes have been developed for a variety of applications, including oxygen enrichment from air, hydrogen purification and air drying. Furthermore, the scales of such application have ranged from less than 2×10^{-3} to more than 1×10^{3} m^3 (STP)/min. Many applications have been reviewed by Cassidy and Holmes (1984), Keller (1983) and Mersmann *et al.* (1984).

Basic theories of PSA involving binary mixtures, which neglect dissipative effects such as intraparticle diffusion and dispersion, and which assume linear adsorption isotherms, have been developed. The trend of their evolution has been towards applicability in increasingly realistic situations. For example, the theories of Shendalman and Mitchell (1972) and Chan *et al.* (1981) are limited to the purification of mixtures in which the more strongly adsorbed (heavy) component is present only at trace impurity levels. Flores Fernandez and Kenney (1983) extended the applicability to arbitrary feed compositions but resorted to numerical integration of some of the relevant equations. Knaebel and Hill (1985) recently developed an analytical solution to the equations governing PSA processes, which is an extension of those earlier theories. Their analysis also applies to the separation of a binary mixture having aribtrary composition. Thus it will be referred to here as the binary, linear isotherm (BLI) theory.

An alternative approach of theoretical analysis has been towards numerical solution of the governing equations. That approach allows inclusion of a variety of dissipative effects, which may be relevant under certain conditions. For example, numerical methods have been developed by Ruthven and co-workers (Hassan *et al.*, 1985; Raghavan and Ruthven, 1985) and by Yang and co-workers (Yang and Doong, 1985; Doong and Yang, 1986) that successfully represent experimental observations. Those models, and preceding models that are mentioned therein, are more comprehensive than the model discussed here, and they may yield greater insight into the fundamental phenomena. Unfortunately, detailed and accurate values of the parameters that describe those effects (such as macropore and micropore diffusivities) are not always available to permit *a priori* predictions of performance. In addition, the theories themselves tend to be rather involved and discourage examination of general trends over broad ranges of operating conditions.

The primary scope of this work is to experimentally test the simple BLI theory, which requires few parameters, but has several constraints that, when met, presumably ensure its validity. Specific goals are to predict the slopes of linear adsorption equilibrium isotherms by applying the theory to dynamic breakthrough experiments, and to test a simple, bench-scale version of the PSA process in order to compare the actual performance with that predicted by the theory. In both cases, conditions are maintained that support the inherent assumptions of the BLI theory.

The BLI theory is applicable to single, dual and multiple column processes. Under certain conditions any of these is capable of producing pure product and therefore may be of considerable interest. Attention is restricted here, however, to the two-column process utilizing a pressurization with product step, as shown in Fig. 1. Another very similar two-column process is known as heatless adsorption (Skarstrom, 1959).

2. SYNOPSIS OF BLI THEORY

Using the method of characteristics to solve the continuity equation, it has been possible to model each step of the PSA process (Knaebel and Hill, 1985). The assumptions and constraints of the theory are listed below.

1. Binary, ideal gas mixture.

†Author to whom correspondence should be addressed.

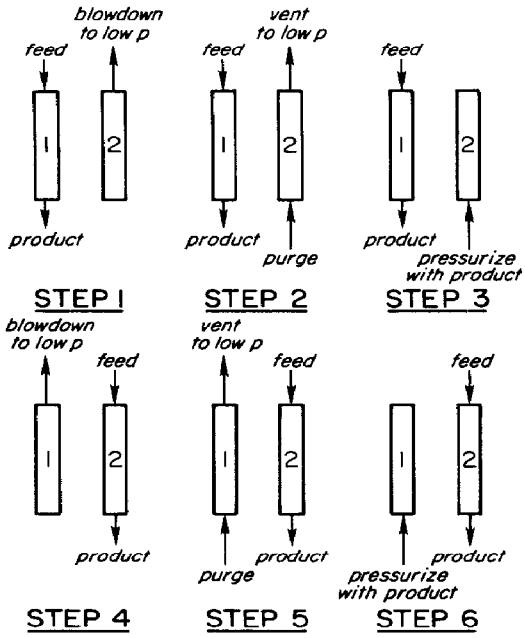

Fig. 1. Six-step, two-bed PSA cycle.

2. Local equilibrium between the gas and solid phases.
3. Linear, uncoupled adsorption equilibrium isotherms.
4. Negligible axial dispersion.
5. Negligible axial pressure gradients.
6. Constant pressure during feed and purge steps.
7. Isothermal operation.
8. No radial dependence in velocity or composition.
9. Identical columns: identical lengths, cross-sectional areas and interstitial void fractions.
10. Complete purification of the light component using the least possible amount of adsorbent.

In order to satisfy the requirement of linear isotherms it was decided to test the adsorption of air on zeolite molecular sieve 5A. It is important to note that the air used in the PSA experiments reported here contains three components: N_2 (78.26 vol.%), O_2 (20.80 vol.%) and Ar(0.94 vol.%). Argon adsorption on molecular sieve 5A from 0 to 60°C and up to 4.67 bar (3500 mm Hg) is essentially identical to that of oxygen. The O_2–Ar pair is therefore treated as a single component and the ternary mixture as a binary.

The high-pressure feed step imposes a square wave change in feed gas composition and proceeds until breakthrough occurs. If the feed gas is enriched in the preferentially adsorbed component (A) and enters a bed whose contents are dilute in that component, then the square wave in composition is maintained along the bed and the effluent gas composition undergoes a square wave shift. The theory predicts this shock phenomenon and the time that it takes the shock to traverse the length of the packed bed. For the case when the packed bed is initially saturated in the less strongly adsorbed component (B) prior to the instantaneous change to a mixed feed gas, the theory states:

$$t_H = t_{SH} = \frac{V_b}{\dot{Q}_{IN}} \gamma_A \tag{1}$$

where

$$\gamma_A = [\varepsilon + (1-\varepsilon)\, k_A]. \tag{2}$$

In the precursor paper (Knaebel and Hill, 1985), the parameter that described the interactions of each adsorbate with the adsorbent bed was $\beta_i = \varepsilon/\gamma_i$.

Rearranging eq. (1) yields the effective isotherm slope

$$k_A = \left(\frac{\dot{Q}_{IN}\, t_{SH}}{V_b} - \varepsilon\right) \frac{1}{1-\varepsilon}. \tag{3}$$

The theory also provides a relation between compositions and volumetric flow rates at two points in the bed:

$$\frac{\dot{Q}_{IN}}{\dot{Q}_{OUT}} = \frac{1 + (\beta - 1)\, y_{OUT}}{1 + (\beta - 1)\, y_{IN}} \tag{4}$$

where

$$\beta = \frac{\varepsilon + (1-\varepsilon)\, k_B}{\varepsilon + (1-\varepsilon)\, k_A} = \frac{\gamma_B}{\gamma_A}. \tag{5}$$

The second specific objective is concerned with the overall performance of the PSA process. An important measure of the effectiveness of a PSA process is the recovery of light component. It is defined as the net product flow rate of the light component divided by the light-component feed rate. For the six-step process of Fig. 1, the BLI theory predicts complete clean-up of the light component and a recovery given algebraically as

$$R_{TH} = (1-\beta)\left(1 - \frac{1}{\mathbf{P}(1-y_F)}\right) \tag{6}$$

where

$$\mathbf{P} = \frac{P_H}{P_L}. \tag{7}$$

It is apparent from the above relations that the properties and interactions of the adsorbates with the packed bed of adsorbent are contained in the terms γ_A and γ_B.

3. EXPERIMENTAL PROGRAM

The relevant properties of the components, parameters that describe the PSA process, and the performance of the process itself were evaluated in a sequence of related experiments. The most fundamental of these, for example, the interstitial void fraction, the particle density and the adsorption isotherms, were determined in separate experiments by simple batch-wise displacement and manometric experiments, respectively. These are described below in Section 3.1.

Subsequently, the results of those experiments were used to interpret independent, cyclic flow experiments in which the effective isotherm slope and PSA recovery of a light component were measured. These experiments are described in Section 3.2.

3.1. *Physical property measurement*

3.1.1. *Void fraction determination.* Simultaneously measuring the interstitial void fraction and the adsorbent bulk density allows calculation of the particle density by the following equation:

$$\rho_p = \frac{\rho_b}{(1-\varepsilon)}. \quad (8)$$

The particle density is a constant for a particular adsorbent, and once it is known, the void fraction can be calculated for any packed bed from the bulk density.

The experimental determination of the void fraction and bulk density, and thus the particle density, was performed using a glass column packed with adsorbent, by the displacement of the voidage of the bed with a suitable liquid. Knowledge of the pertinent empty volumes, weights and liquid density enabled calculation of the void fraction.

The adsorbent was 5A zeolite molecular sieve (Union Carbide 20 × 40 mesh). Cyclohexane was used as the displacement fluid since its large molecular diameter prevented it from entering the so-called α and β cages of zeolite. The void fraction comprised all the voids outside the zeolite crystal lattice relative to the total bed volume. This definition is practically equivalent to the fluid mechanical definition, allowing calculation of the interstitial velocity. To test the hypothesis that cyclohexane is excluded from the zeolite crystal, n-octadecane (n-$C_{18}H_{38}$) was used in an identical experiment. It is reasonable to assume that neither cyclohexane nor n-octadecane significantly penetrates the zeolite crystal lattice because their approximate collision diameters are 6.2 and 8.6 Å, respectively. In all the experiments the displacement liquid was degassed and admitted slowly to the apparatus to minimize bubble formation and entrained air in the packed bed during filling.

3.1.2 *Equilibrium isotherm measurements.* It is known that at 24°C oxygen exhibits linear isotherm behaviour on zeolite molecular sieve 5A up to 5.33 bar (4000 mm Hg), while nitrogen adsorption is approximately linear only to 0.2 bar (150 mm Hg) (Miller *et al.*, 1986). To study the BLI theory at higher nitrogen partial pressures than 0.2 bar (150 mm Hg), however, it was necessary to ensure that nitrogen adsorption was linear at higher pressures. Consequently, adsorption isotherms were measured at elevated temperatures.

The existence of uncoupled isotherms, such that the adsorption of each component depends only on its own partial pressure, has been shown to be a good assumption for the nitrogen–oxygen binary on molecular sieve 5A at 24°C and partial pressures up to at least 2.67 bar (2000 mm Hg) (Miller *et al.*, 1986). Coupling was assumed negligible in this study, which was reasonable since the temperatures employed were even greater than 24°C. As a result, only pure component isotherm measurements were deemed necessary.

Adsorption of nitrogen and oxygen on zeolite was measured by a manometric technique. The individual isotherms were measured at 30, 45 and 60°C at pressures up to 4.67 bar (3500 mm Hg) to determine the range over which the isotherms could be taken as linear (Kayser, 1985).

It is important to note that the particle density determined by the void fraction experiment is required to interpret the isotherm measurements. Therefore, a consistent value of particle density was obtained and used. Conversely, for a given packed bed (i.e. of known volume and mass of adsorbent), the value of γ_i is independent of the particle density and void fraction, as long as they are consistent with the measured isotherm slope. In this respect, to be useful for adsorber design or analysis according to the present theory, isotherm data should be obtained with the measured or assumed particle density, and the value of the void fraction determined from the bulk and particle densities should be used to estimate the values of γ_i. Disparate definitions may lead to erroneous results.

3.2. *Experimental evaluation of the BLI theory*

3.2.1. *Breakthrough experiments.* The utility and interpretation of simple breakthrough experiments are well known (Sherwood *et al.*, 1975). In PSA applications such experiments also provide guidance in selecting individual step times. Thus an apparatus, shown in Fig. 2, was assembled for the sole purpose of extracting effective isotherm slopes. In addition, data obtained in preliminary PSA experiments, which were intended to identify appropriate step times, were also used to evaluate effective isotherm slopes. The latter apparatus and experiments are described in Subsection 3.2.2.

Operation of the breakthrough apparatus involved switching the feed gas from pure B to pure A at the

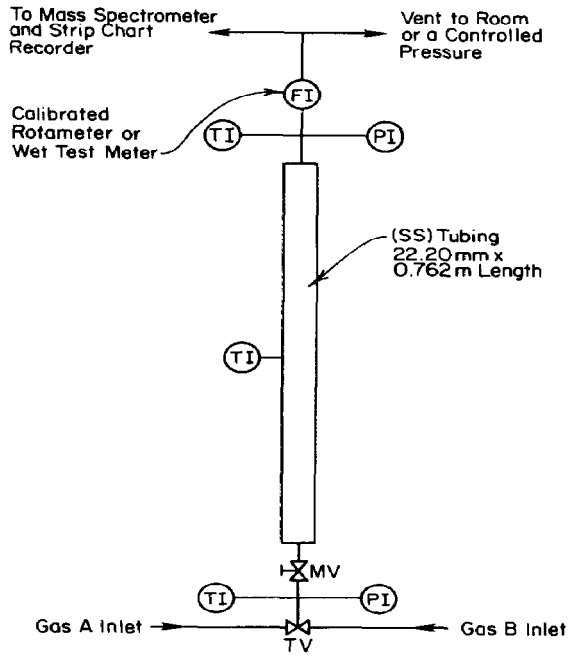

Fig. 2. Diagram of apparatus used for breakthrough studies.

outset of an experiment. Simultaneously, the effluent composition and flow rate were monitored. Preliminary experiments were conducted to evaluate the distance–velocity lag of the dead volume and response time of the instruments. Ultimately, the time necessary for the composition shock-front to traverse the adsorbent bed was obtained. This value was used in eq. (3) to estimate the effective slope of the adsorption isotherm. Note that, according to eq. (4), measurement of both the influent and effluent volumetric flow rates allows direct determination of the parameter, β.

3.2.2. *PSA experiments.* The PSA experimental apparatus is shown schematically in Fig. 3. The network of solenoid valves was designed to accommodate the six-step cycle (cf. Fig. 1). The actual valve sequence is listed in Table 1. Other aspects of the design (e.g. the bed geometry) and operating conditions (e.g. throughput and pressure ratio) were manipulated in order to correspond with the assumptions and constraints listed in Section 2.

To illustrate, Fig. 4 shows the ideal, theoretical pressure profile and a typical profile as it actually occurred. The minor deviations between these are due to surges associated with valve switching, finite pressure drop in the adsorbent bed and fittings, and

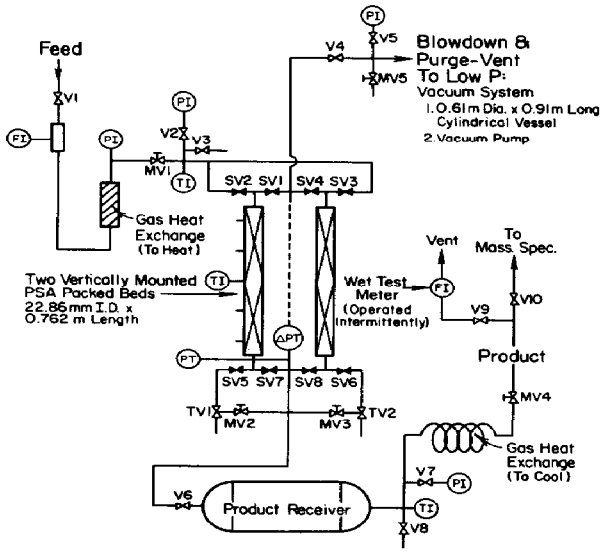

Fig. 3. Two-bed PSA process diagram.

Table 1. Solenoid valve positions for the six-step cycle

Step	Valves open
1	2, 4, 7
2	2, 4, 6, 7
3	2, 7, 8
4	1, 3, 8
5	1, 3, 5, 8
6	3, 7, 8

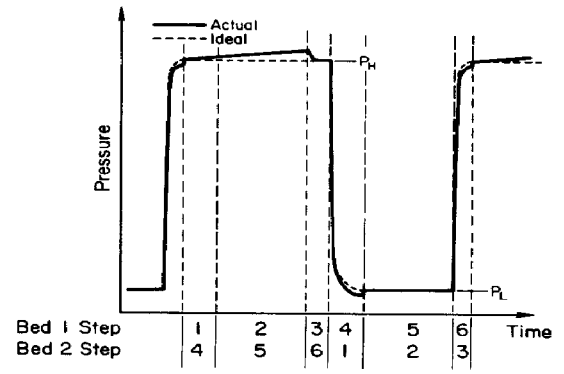

Fig. 4. Ideal and actual pressure-vs.-time profiles for PSA cycles.

finite reservoir capacities. The molar feed rate was set by operating MV1 under critical flow conditions, with constant upstream pressure and temperature. Critical flow ensured that pressure fluctuations downstream of MV1 did not affect the molar feed rate. The product flow through MV4 also occurred in the critical regime, but the flow rate was only approximately constant because the pressurization step caused the pressure in the product receiver (and in the alternative column) to drop (see Fig. 4). Consequently, the critical flow through MV4 varied since it was proportional to the upstream pressure. The observed drop in the pressure was less than 3% for all experiments because of the large volume of the product receiver. Since the pressure of the receiver dropped during each pressurization step, it increased during the other steps. The product valve, MV4, was set at the beginning of an experiment to allow the pressure to increase properly after a pressurization step. Furthermore, since the pressure fluctuations in the product receiver were small, the product flow rate varied only slightly. A wet test meter was used to monitor the product flow over several cycles to ensure that an accurate mean was obtained.

In Fig. 4 it is evident that there was actually a pressure increase in a given bed when switching from the blowdown to purge steps. A similar increase also occurred when switching from the pressurization to high-pressure feed steps. The increase was attributable to the pressure drop induced by the purge and feed flows. Only for purge steps occurring below 0.34 bar (260 mm Hg) did the total pressure drop exceed 10% of the inlet pressure. For the high-pressure feed step, the total bed pressure drop was about 1% of the inlet pressure for all of the conditions studied. The assumption in the theory of negligible pressure drop was not always valid but calculations were performed using the average bed pressure with little loss in accuracy.

3.2.3. *Operating procedures.* The operating procedures were strongly influenced by the assumptions inherent in the BLI theory. First of all, the high-pressure feed step proceeded until the composition shock reached the end of the bed in order to ensure

complete adsorbent utilization. Similarly, during the purge step the minimum amount of product gas was used to purge the heavy component from the bed. Likewise, slow cycling of the pressure led to low interstitial gas velocities, which supported the assumptions of the theory. In addition, the other premises of local equilibrium, negligible axial dispersion and negligible pressure drop were all favoured by slow cycling.

The cycle time was selected in order to operate the process with constant feed rate, i.e. to satisfy the following equation:

$$t_H = t_{BD} + t_L + t_{PR}. \quad (9)$$

The time of the high-pressure feed step, t_H, was measured for any given feed rate by a breakthrough experiment, as described earlier ($t_H = t_{SH}$). Similarly, the times for blowdown and purge, t_{BD} and t_{PR}, were measured experimentally. It was important to minimize $t_{BD} + t_{PR}$ so t_L could be as large as possible. This allowed the purge flow rate to be as small as possible, resulting in a minimal pressure drop during the purge step. Breakthrough experiments were performed at different purge flow rates until the proper flow rate was determined, i.e. to purge the bed completely during t_L.

The step times were all predetermined for a given feed rate, feed pressure and pressure ratio. MV1, MV2 and MV3 were tuned to deliver the desired flows by calibration with a wet test meter.

To ensure that the process was operated at the limit (i.e. without excess capacity), the following start-up procedure was used. The feed rate used to calculate t_H was reduced but t_H was maintained so that the composition shock did not reach the end of the bed during the feed step. Additionally, the pressure of the blowdown and purge steps was reduced below the value used to set purge valves. This ensured that the purge was adequate to remove the heavy component thoroughly.

Finally, prior to start-up the process was purged with light component at the desired high pressure, and the entire apparatus was heated to the desired temperature. The solenoid valves were operated synchronously by a computer with predetermined step times.

During start-up a pure product was produced but the recovery was not the maximum achievable. When start-up was not overly conservative and the pressure ratio was great enough to ensure positive recovery, the process could be tuned. First, the feed rate was increased slowly, until heavy component appeared in the product, then it was reduced to a value just below that. In this manner, the composition shock was allowed to reach the end of the column. Second, the pressure during the purge and blowdown steps was increased until heavy component appeared in the product. This gave the minimal purge flow, so that the composition simple-wave just reached the feed end of the bed.

During the tuning steps above, the product valve, MV4, was adjusted to ensure that the pressure in the product receiver was maintained at the desired level. Finally, MV4 was set to ensure that the cycle-to-cycle pressure was constant.

After the steps above were completed, the process was operated for several hours (often overnight) to ensure that steady-state conditions were attained. This was required because of the slow dynamics of the large product receiver. Once steady state was reached, data were recorded hourly for several hours.

4. RESULTS

4.1. *Physical properties of the adsorbent*

Table 2 summarizes the results of the void fraction experiments. The data indicate that a consistent void fraction was measured with n-octadecane and cyclohexane for molecular sieve 5A.

Nitrogen and oxygen isotherms were measured at 30, 45 and 60°C. The 45°C data are presented in Fig. 5. Table 3 is a summary of the subsequent linear regression results.

As Fig. 5 indicates, the nitrogen isotherm at 45°C is approximately linear for the pressure range studied. The oxygen isotherms are linear for the entire range of temperatures and pressures studied.

Table 2. Void fraction measurements on zeolite 5A

Run	Liquid	ε
1	C_6H_{12}	0.492
2	C_6H_{12}	0.477
3	C_6H_{12}	0.463
4	C_6H_{12}	0.476
5	n-$C_{18}H_{38}$	0.481
		$\bar{\varepsilon} = 0.478 \pm 0.010$

$\rho_b = 810.0 \pm 2.0\,kg/m^3$; $\rho_p = 1552.0 \pm 30.0\,kg/m^3$.

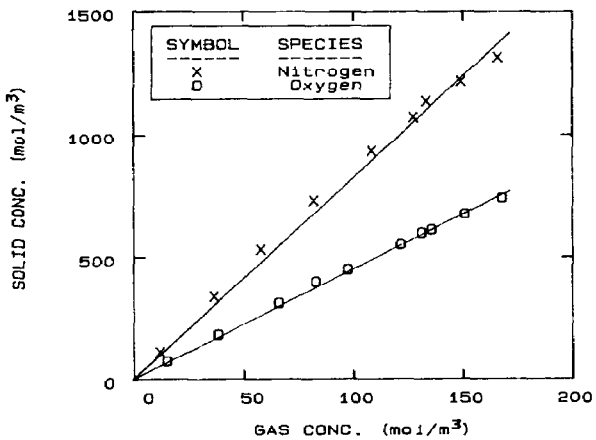

Fig. 5. Equilibrium isotherms of nitrogen and oxygen on zeolite 5A at 45°C. The lines represent linear regression results.

Table 3. Linear regression of equilibrium data

Gas	T (°C)	k_i
N_2 (A)	30	9.94
N_2 (A)	45	8.24
N_2 (A)	60	7.55
O_2 (B)	30	5.40
O_2 (B)	45	4.51
O_2 (B)	60	3.723

i = A or B. k_i is dimensionless.

4.2. *Experimental test of the BLI theory*

4.2.1. *Breakthrough experiments.* Table 4 represents the results of six breakthrough experiments. These were determined from composition and flow data according to eq. (3). The agreement between the values obtained by breakthrough experiments and equilibrium experiments is quite good. The PSA apparatus exhibited slightly less variance for the breakthrough experiments than did the single column breakthrough unit, as Table 4 indicates.

4.2.2. *PSA experiments.* The BLI theory predicts complete clean-up of the light component and recovery of the light component given by eq. (6). Therefore, it is appropriate to compare the experimentally measured values with those predictions. The experimentally determined recovery of the light component for the PSA process of Fig. 3 is simply the ratio of the net product rate of light component divided by the feed rate of light component. In this study, β and **P** were varied while y_F was constant in all experiments. The parameter, β, depended on the equilibrium adsorption isotherm slopes, which are listed in Table 3, and was weakly temperature-dependent, equalling 0.593 at 45°C and 0.548 at 60°C. The pressure ratio, **P**, was varied by adjusting the blowdown and purge pressure, i.e. P_L. The blowdown pressure was varied by controlling the pressure of the vacuum receiver vessel, which was attached to a vacuum pump. Table 5 summarizes all of the PSA recovery results, and values at 45°C are shown in Fig. 6.

Table 6 is a list of typical step times used in the PSA studies. Procedures, equipment, calculations and statistical information for each experiment are summarized elsewhere (Kayser, 1985).

5. DISCUSSION

The experimental data indicated the BLI model (based on binary, linear isotherms) was accurate for the experimental conditions tested. Application of the theory to breakthrough experiments enabled predic-

Table 4. Equilibrium isotherms from breakthrough experiments

Binary	Method†	P (bar)	T (°C)	u_{IN} (m/s)	$k_{A_{BR}}$	$k_{A_{EQ}}$	$\Delta\%$‡
N_2 (A)–O_2 (B)	1	0.229	24	0.1420	23.66	23.62§	+0.2
N_2 (A)–O_2 (B)	2	3.116	45	0.0748	8.59	8.24	+4.2
N_2 (A)–O_2 (B)	2	3.023	60	0.0640	7.22	7.55	−4.4
O_2 (A)–Ar (B)	1	1.000	20	0.0388	7.21	6.94§	+3.9
O_2 (A)–Ar (B)	1	1.002	45	0.0424	4.99	4.51	+10.6
O_2 (A)–Ar (B)	1	1.004	60	0.0444	4.05	3.723	+8.8

†Method 1: Using apparatus of Fig. 2; the mass of adsorbent was 0.2399 kg. Method 2: PSA system of Fig. 3; the mass of adsorbent in each column was 0.2524 kg.
‡Average absolute $\Delta\% = 5.4$.
Note: $\Delta\% = (k_{A_{BR}} - k_{A_{EQ}}) \times 100/k_{A_{EQ}}$
§Equilibrium isotherm slope extracted from the data of Miller (1984).
u_{IN} was calculated at the average bed pressure following breakthrough, based on the volumetric flow rate, $\dot{Q}_{IN} = \varepsilon A_{CS} u_{IN}$.

Table 5. PSA recovery data of O_2 + Ar from air

Run†	P_H (bar)	P	T (°C)	(O_2 + Ar) product (vol.%)	Q_{IN} (l (STP)/min)	R_{EXP}	R_{TH}	$\Delta\%$
1	3.085	6.476	45	99.72	2.342	0.10174	0.1179	+15.9
2	3.133	7.695	45	99.74	2.342	0.1838	0.1637	−10.9
3	3.122	12.36	45	99.75	2.333	0.2870	0.2556	−10.9
4	3.029	23.54	45	99.80	2.314	0.3294	0.3275	−0.6
5	3.143	803§	45	99.27	2.344	0.4067	0.4047	−0.5
6	3.023	840§	60	99.34	1.851	0.4332	0.4492	+3.7

†Each run represents the average of 2–6 h of data collection at steady state.
‡Average absolute $\Delta\% = 7.1$. Note: $\Delta\% = (R_{TH} - R_{EXP}) \times 100/R_{EXP}$.
§For runs 5 and 6, the large pressure ratio was obtained by operating at a blowdown pressure of less than 0.0040 bar (3 mm Hg). For these runs a purge step was not necessary.
The mass of adsorbent in each column was 252.4 g. $\beta = 0.593$ at 45°C; $\beta = 0.548$ at 60°C.

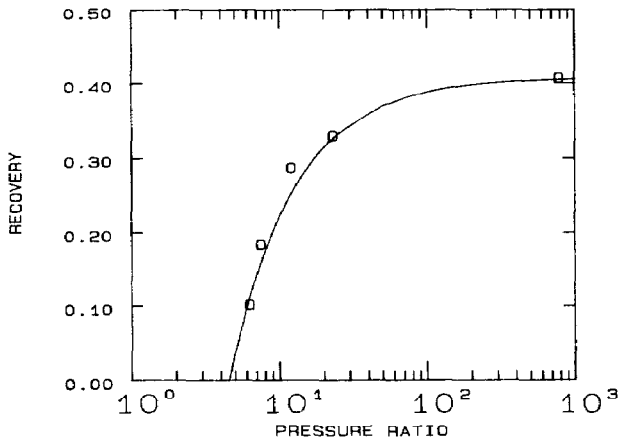

Fig. 6. Theoretical (curve) and experimental (O) oxygen recoveries at 45°C.

Table 6. Typical cycle times (runs 1–4)

Step	Time (s)
1	35
2	65
3	5
4	35
5	65
6	5
Total	210 s

Cf. Table 1 for valve sequencing.

tion of the slope of linear equilibrium isotherms with an average absolute error of 5.4% relative to batch-wise equilibrium values. The theory predicted the light component recovery of a PSA process with an average absolute error of 7.1% relative to experimental values, over a pressure ratio range of 6.5 to 840. Furthermore, the theory predicted that complete clean-up of the light component was achievable, while the light-component product purity in the laboratory was never less than 99.2 vol.% and averaged 99.6 vol.%. The differences between the theory and the experiments were attributed to experimental error, minor violations of the assumptions and constraints of the theory, and imperfect mechanical design.

Although the apparatus and conditions studied here were selected to evaluate the BLI theory, the close correspondence between the theory and experimental results suggests that the theory may be applicable to the design of some types of commercial-scale PSA processes. The theory provides a means for estimating the slopes of the adsorption isotherms and the parameter, β, which has signal influence on recovery. The only other requisite data are the void fraction and adsorbent density. These values must be consistent with the isotherm slopes, but deviations from true values are of little consequence.

One course for gaining increased understanding of PSA systems is to explore the limitations of the present theory, perhaps to examine conditions when the assumptions of the theory are clearly violated, to see whether behaviour is consistent with the general trends predicted by the theory. Further studies are planned to examine the effects of nonlinear isotherms, faster cycling and increased throughput, and temperature and pressure variations on the separation of air and other mixtures.

Acknowledgements—The authors are grateful to the U.S. Air Force School of Aerospace Medicine and the Southeastern Center for Electrical Engineering Education for supporting this work. In particular, the support of Dr. Kenneth G. Ikels was invaluable. This research was sponsored by the Air Force Office of Scientific Research/AFSR United States Air Force, under Contract F49620-82-C-0035. The United States Government is authorized to reproduce and distribute reprints for governmental purposes notwithstanding any copyright notation hereon.

NOTATION

A_{CS}	cross-sectional area of bed, m^2
k_i	slope of equilibrium isotherm of component i, dimensionless
k_{EQ}	slope of isotherm determined in batch-wise experiments
k_{BR}	slope of isotherm measured in column breakthrough experiments
L	length of column, m
P	PSA cycle pressure ratio = P_H/P_L
P_H	average bed pressure during high-pressure feed, bar
P_L	average bed pressure during low-pressure purge, bar
$\dot{Q}_{IN}$	volumetric flow rate of feed, l/min at a given T and P
$\dot{Q}_{OUT}$	volumetric fow rate of feed, l/min at a given T and P
R	recovery, $\frac{\text{product B}}{\text{feed B}}$
R_{EXP}	experimental recovery
R_{TH}	theoretical recovery
t_{BD}	time for the blowdown step, s
t_H	time for the high-pressure feed step, s
t_L	time for the low pressure-purge, s
t_{PR}	time for the pressurization step, s
t_{SH}	time for the composition shock to traverse a bed, s
T	temperature, K or °C
u_{IN}	interstitial velocity of the feed gas to a column, m/s
V_b	volume of column of adsorbent, m^3
y_E	mole fraction of A in the effluent product gas
y_F	mole fraction of A in the feed gas

Greek letters

β	separation factor defined by eq. (5)
γ_i	adsorbent bed parameter for component i defined by eq. (2)
ε	adsorbent bed void fraction

ρ_b bulk density, kg/m^3
ρ_p particle density, kg/m^3

REFERENCES

Cassidy, R. T. and Holmes, E. S., 1984, Twenty-five years of progress in "adiabatic" adsorption processes. *A.I.Ch.E. Symp. Ser.* **80**, 68–75, 233.

Chan, Y. N. I., Hill, F. B. and Wong, Y. W., 1981, Equilibrium theory of a pressure swing adsorption process. *Chem. Engng Sci.* **36**, 243–251.

Doong, S. J. and Yang, R. T., 1986, Bulk separation of multicomponent gas mixtures by pressure swing adsorption: pore/surface diffusion and models. *A.I.Ch.E. J.* **32**, 397–410.

Flores Fernandez, G. and Kenney, C. N., 1983, Modelling the pressure swing air separation process. *Chem. Engng Sci.* **38**, 827–834.

Hassan, M. M., Raghavan, N. S., Ruthven, D. M. and Boniface, H. A., 1985, Pressure swing adsorption, II: experimental study of a nonlinear trace component isothermal system. *A.I.Ch.E. J.* **31**, 2008–2016.

Kayser, J. C., 1985, Pressure swing adsorption: experimental analysis of the method of characteristics theoretical model. M.S.Ch.E. Thesis, The Ohio State University.

Keller, G. E., II, 1983, Gas adsorption processes: state of the art in industrial gas separations. *Am. Chem. Soc. Symp. Ser.* **223**, 145–169.

Knaebel, K. S. and Hill, F. B., 1985, Pressure swing adsorption: development of an equilibrium theory for gas separations. *Chem. Engng Sci.* **40**, 2351–2360.

Mersmann, A., Munstermann, U. and Schadl, J., 1984, Separation of gas mixtures by adsorption. *Ger. chem. Engng* **7**, 137–149.

Miller, G. W., Knaebel, K. S. and Ikels, K. G., 1986, Adsorption equilibria of nitrogen, oxygen, argon, and air on zeolite 5A. *A.I.Ch.E. J.* to be published in December issue, 1986.

Raghavan, N. S. and Ruthven, D. M., 1985, Pressure swing adsorption, III: numerical simulation of a kinetically controlled bulk gas separation. *A.I.Ch.E. J.* **31**, 2016–2025.

Shendalman, L. H. and Mitchell, J. E., 1972, A study of heatless adsorption in the model system CO_2 in He—I. *Chem. Engng Sci.* **27**, 1449–1458.

Sherwood, T. K., Pigford, R. L. and Wilke, C. R., 1975, *Mass Transfer*. McGraw-Hill, New York.

Skarstrom, C. W., 1959, Use of phenomena in automatic plant type gas analyzers. *Ann. N. Y. Acad. Sci.* **72**, 751–763.

Yang, R. T. and Doong, S. J., 1985, Gas separation by pressure swing adsorption: a pore diffusion model for bulk separation. *A.I.Ch.E. J.* **31**, 1829–1842.